ECS Journal of Solid State
Science and Technology

The Electrochemical Society
Advancing solid state & electrochemical science & technology

# Synergetic Effect of 1,2,4-triazole and Glycine on Chemical Mechanical Planarization of Aluminum at Low Polishing Pressure in an Eco-Friendly Slurry

To cite this article: Ping Sun *et al* 2020 *ECS J. Solid State Sci. Technol.* **9** 034003

View the article online for updates and enhancements.

You may also like

- Characterization of 1, 2, 4-Triazole as Corrosion Inhibitor for Chemical Mechanical Polishing of Cobalt in $H_2O_2$ Based Acid Slurry
Peng He, Bingbing Wu, Shuai Shao et al.

- Controlling the Removal Rate Selectivity of Ruthenium to Copper during CMP by Using Guanidine Carbonate and 1, 2, 4-Triazole
Qingwei Wang, Jianwei Zhou, Chenwei Wang et al.

- Role of 1,2,4-Triazole as a Passivating Agent for Cobalt during Post-Chemical Mechanical Planarization Cleaning
Mingjie Zhong, Shyam S. Venkataraman, Yongqing Lan et al.

This content was downloaded from IP address 110.65.147.241 on 21/03/2023 at 07:04

*ECS Journal of Solid State Science and Technology*, 2020 **9** 034003
2162-8777/2020/9(3)/034003/9/$40.00 © 2020 The Electrochemical Society ("ECS"). Published on behalf of ECS by IOP Publishing Limited

# Synergetic Effect of 1,2,4-triazole and Glycine on Chemical Mechanical Planarization of Aluminum at Low Polishing Pressure in an Eco-Friendly Slurry

**Ping Sun,[1] Yongguang Wang,[1,z] Ping Liu,[2] Yuguang Zhu,[1] Yongwu Zhao,[2] Dong Zhao,[1,z] and Hui Deng[3]**

[1] *School of Mechanical and Electric Engineering, Soochow University, Suzhou, Jiangsu 215021, People's Republic of China*
[2] *School of Mechanical Engineering, Jiangnan University, Wuxi 214122, People's Republic of China*
[3] *Department of Mechanical and Energy Engineering, Southern University of Science and Technology, Shenzhen, Guangdong 518055, People's Republic of China*

In this paper, glycine and 1,2,4-triazole (TAZ) are used as eco-friendly additives to compensate the decrease in removal rate owing to the low polishing pressure in chemical mechanical planarization (CMP) of aluminum (Al) at near-neutral pH value. It demonstrated that the synergetic effect of glycine and TAZ participates in the formation of a weak passive layer with the hardness of 0.419 GPa on Al surface, which is compact enough to protect the Al surface from chemical dissolution and meanwhile relatively weak enough to achieve high polishing rate. Even at a low polishing pressure of 1.0 psi, a material removal rate of 750 nm $min^{-1}$ with surface roughness of 0.19 nm was obtained in an eco-friendly slurry at pH 7.5. It was found that the weak passive layer is physicochemical formed on surface of Al with Al-TAZ bonds, which is subsequently complexed by glycine with Al-COOH bonds verified by Langmuir isotherm theory and X-ray photoelectron spectroscopy test. The above two synergistic parts are integrated into the material removal process. The material planarization mechanism in CMP process of Al was discussed as well.
© 2020 The Electrochemical Society ("ECS"). Published on behalf of ECS by IOP Publishing Limited. [DOI: 10.1149/2162-8777/ab7882]

Manuscript submitted December 9, 2019; revised manuscript received February 11, 2020. Published February 28, 2020.

In order to reduce the leakage current because of short channel effect, metal gate/high-k stacks have been widely used in sub-45 nm technology node of complementary metal-oxide-semiconductor (CMOS).[1,2] Intel firstly proposed an approach of high-k metal gate (HKMG) integrated with a replacement meatal gate (RMG) for the 45 nm technology node.[3,4] Subsequently, IBM developed an Al-Co gate to effectively reduce the gate length to 11 nm.[2] As the feature size shrinks down to 28 nm and below, aluminum (Al) is commonly used in front-end-of-line (FEOL) structures as a feasible gate material.[5,6] Damage-free and atomically smooth surface of Al is required in the "gate-last" integration scheme for HKMG transistors. In addition, in the fabrication process of FinFET devices, the RMG gate material includes tungsten (W), aluminum (Al), nickel (Ni), cobalt (Co), and titanium (Ti).[7,8] Tungsten has also been widely used as a plug material in multi-level interconnection structure contact during middle of line (MOL) in various contemporary memory devices, such as NAND flash memory and dynamic random access memory (DRAM).[9] Therefore, the optimization of W CMP slurry is also an important research topic.

It is well known, the conventional chemical mechanical planarization (CMP) with high polishing pressure is considered as an essential technique in fabrication of multilevel interconnections of microchips and electronic devices to achieve both local and global planarization. Nonetheless, the HKMG structure containing porous and fragile materials results in a new requirement of low polishing pressure (~1 Psi) during CMP of Al, to avoid the fracture of HKMG structure in the CMP process because of its low mechanical strength.[6,10–12]

Over the past few decades, CMP mechanism of Al has been intensively studied in aqueous solution with high polishing pressure.[13] Most of previous studies focused on the process of Al CMP in both acidic and alkaline media according to the Pourbaix diagram of Al.[10,14–19] However, the drawback of this normal process is application of strong acids or alkalis in the CMP process, which leads to large quantity of wastewater with high solid content and turbidity.[20] It remains a challenge and highly desirable to develop a novel slurry for Al CMP consisting of non-hazardous chemicals at near-neutral pH value, since environment-friendly slurry could lead to improved topography and lower defectivity. Several researches regarding developing eco-friendly Al CMP polishing slurry have been reported. From the study of Wang,[2] synergistic effect of glycine and TT-LYK can effectively control galvanic corrosion control between Al-Co interface in alkaline slurry. Wang et al.[10] investigated the influence of glycine and pH on Al CMP performance using electrochemical techniques. Besides, polishing slurries, which are applied for other metal CMP processes like copper CMP, also have important reference value for this study.[20–22] One challenge for CMP in the neutral pH region is the chelating efficiency of complexation compounds because they prefer soluble $Al^{3+}$ in contrast to the insoluble $Al_2O_3$ layer in the neutral pH regime.

In order to satisfy the above requirements, a proper slurry formulation with dual functions is significantly demanded to compensate the low polishing pressure in CMP of Al.

On one hand, the mechanical shear stress on Al surface should be reduced in CMP process to avoid the fracture of HKMG structure.[6,11,12,23] According to the Preston theory,[24] it is noticeable that the decrease in polishing pressure leads to the decrease in material removal rate in Al CMP process.[25] Therefore, a chemical film on the Al surface in CMP process should be relatively weak enough to realize high material removal rate at low polishing pressure, and meanwhile be dense enough to protect the Al surface from chemical dissolution. As well acknowledged, glycine as an effective complexing agent is commonly employed to compensate the decrease of removal rate resulting from low polishing pressure.[2,26,27]

On the other hand, an environmental-friendly slurry of Al at near-neutral pH value is also required to eliminate the toxic and strong acids or alkalis in CMP process.[28] Currently, benzotriazole (BTA) is most widely used as an inhibitor to achieve high surface quality in Al CMP process,[22,29,30] and its corresponding passivation mechanism has been intensively investigated as well.[16] Nevertheless, BTA is toxic and poor decomposition, which creates disposal issues of the toxic chemicals in CMP process.[31–34] In addition, it is reported that the removal of BTA passive film on Al surface requires a strong mechanical force, which cannot be easily removed as the polishing pressure is low as ~1 Psi in Al CMP process.[6,20] Moreover, the unremoved BTA residue will also lead to serious organic contaminants.[6,35] Interestingly, 1,2,4-triazole (TAZ) with a variety of covalent bond interactions could be consider as a week inhibitor compared with BTA, which is easy to be biodegraded and will be a

zE-mail: wangyg@suda.edu.cn; zhaodong@suda.edu.cn

promising weakly inhibitor in Al CMP process at low polishing pressure.[6,20,22,34] However, to our knowledge, the interaction between TAZ and glycine on the Al CMP performance has not been well investigated and revealed.

In this paper, a novel CMP process of Al is proposed in an eco-friendly slurry at near-neutral pH value. The synergetic effects of glycine and TAZ on material removal at low down pressure for CMP of Al were investigated by using atomic force microscope (AFM), electrochemical polarization tests, nano-indentation and X-ray photoelectron spectroscopy (XPS).

## Experimental

***CMP slurry preparation.***—The main additives used in polishing slurry were colloidal silica (30 nm, the mass fraction of 10%) as an abrasive, hydrogen peroxide ($H_2O_2$) as an oxidizer, hydroxyethyl cellulose (HEC) as a surfactant, glycine as a complexing agent, TAZ as a corrosion inhibitor, a designated amount of the above chemicals was mixed with deionized water (DI) based on the experimental requirement. The pH value of the slurry was adjusted to 7.5 by hydrochloric acid (HCl) and triethanolamine. The Al weight was measured before and after polishing to calculate the material removal rate using a precision electronic balance (Mettle Toledo XS205-DU, the precision is $\times 10^{-5}$g). To ensure the reliability of the data, each polishing test was repeated 3 times and each tested sample was weighed several times to get an average value. The usage of all reagents was of analytical grade.

***Polishing experiments.***—99.99 wt% pure Al samples (20 × 20 × 1 mm) were polished on a UNIPOL-1200 s polisher (Shenyang Kejing Auto Co., Ltd.) with the following process parameters: working pressure 1.0 psi, head speed/plate speed 60 rp m/60 rpm. The Al sheet was ground by 240 #∼1600 # metallographics paper prior to the polishing tests.

***Static dissolution rate experiments.***—In order to investigate the chemical dissolution of Al in CMP polishing slurry, the Al sheets were immersed in different kinds of polishing slurry for 3 min. The inhibition efficiency $\theta$ is derived by calculation of weight loss according to Eq. 1.

$$\theta = \frac{w_a - w_p}{w_a} \times 100\% \qquad [1]$$

Where $w_a$ and $w_p$ are the weight loss with and without corrosion inhibitor, respectively.

***Electrochemical test-dynamic and static.***—In situ open circuit potential (OCP) and potentiodynamic polarization test were employed on Al panels to study the mechanism of Al dissolution in different polishing slurries. A CHI660E electrochemical workstation (Shanghai Chenhua Instrument Co., Ltd.) with a three electrode cell was used.

A commercial mercury electrode and a platinum mesh were referred to as the reference and counter electrodes, respectively. An aluminum encased in epoxy resin was applied as the working electrode. Prior to the measurement, the aluminum electrode was firstly immersed into 0.04 wt% $HNO_3$ for 1 min to remove the native passive films. The exposed area was 4 $cm^2$. A certain period before data acquisition, i.e. 1 h, is required for immersion of Al electrode into the prepared polishing slurry to achieve a stable state. The scanning speed and the scanning sensitivity was 5 mv $s^{-1}$ and $10^{-6}$ A $V^{-1}$, respectively. On the average, three replicated samples were tested for each condition. More details of the in situ OCP preparation can be found elsewhere.

***Electrochemical impedance spectroscopy measurements (EIS).***—EIS with a SR810 frequency response analyzer connected to a Gamry CMS100 potentiostat was performed to corrosive tests of inhibitor-treated samples in different polishing slurries. The measured frequency range was from $10^{-2}$ to $10^5$ Hz, with an AC excitation amplitude of 10 mV. The reference electrode of Ag-AgCl was applied and coupled with a platinum counter electrode. The exposed surface area was 4 $cm^2$.

***Surface characterization.***—The morphology of the Al sheet was characterized by CSPM5000 atomic force microscope (AFM, Benyuan Co., Ltd., China) with SiN tip of a radius of 180 nm during in situ tapping model at a scanning area of 10 × 10 $\mu$m. The diverse valence state of elements on specimens was identified by XPS (AXIS-ULTRA DLD, Kratos, Japan). XPS test was carried out by an Al K$\alpha$ radiation source (1486.6 eV) at 15 KV anode with 17 mA emission current. The binding energies were calibrated against the binding energy of C 1s. And the corresponding measured scale was 700 × 300 $\mu$m.

***Hardness test.***—The Hardness and elastic modulus of Al-TAZ film was examined by nanoindentation tests. Instrumented nanoindentation experiments were conducted using TI950-PREMIER tester (HYSITRON, Inc., USA) with and without TAZ. The applied load was increased from 0 mN to 1 mN quadratically (10 s loading/unloading time). Separate locations were performed individual indentations on Al-TAZ film. A postscan with scanning area of 10 × 10 $\mu$m at a normal force of 2 $\mu$N was applied to acquire surface information of the indentation.

## Results and Discussion

***Effect of glycine concentration on the polishing of aluminum.***—With the based polishing slurry (10 wt% colloidal silica, 0.05 wt% HEC, 0.6 wt% $H_2O_2$, pH = 7.5), different glycine concentrations were mixed with the above based slurry. The effect of glycine on Al removal rate is shown in Fig. 1a. It is found that the increase in glycine concentration leads to the sharply increase in removal rate at low concentration of glycine, and the further increase in glycine results in the gradually increase in removal rate. This observation is consistent with the published experimental data.[10,36] It is reported that glycine molecules can be complexed with metal ions, such as Al ion and Al oxide to produce glycine-Al soluble products.[2] At low glycine concentration, the chelating rate is facilitated by the addition of more glycine in the slurry, contributing to the dramatically increase in material removal rate. However, the unreacted surface is effectively all occupied and the further increase in glycine content could not find any more surface molecules to react at high glycine concentration.[36]

Figures 1b–1d indicates the morphology of the specimen after polishing with glycine. The surface in Figs. 1b and 1c appears relatively smoother. It is observed etch pits and corrosive tracks in Fig. 1d. The surface roughnesses (Ra) in Figs. 1b, 1c and 1d are 2.01 nm, 2.61 nm and 4.87 nm respectively. It can be estimated that an inhibitor is required to reduce the corrosion of glycine in CMP of Al, although the addition of glycine could enhance the removal rate. The desirable surface quality of Al surface after CMP is inferred to be depended on achieving synergy between glycine and inhibitor.

***Synergistic effect of TAZ and glycine on aluminum CMP.***—As listed in Table I, additives with variable concentrations were mixed

**Table I. Five kinds of slurry with different contents of glycine and TAZ.**

| Slurry | Slurry addition |
|---|---|
| A | 1 wt% glycine+10 mmol $l^{-1}$ TAZ + based polishing slurry |
| B | 1 wt% glycine+20 mmol $l^{-1}$ TAZ + based polishing slurry |
| C | 2 wt% glycine+20 mmol $l^{-1}$ TAZ + based polishing slurry |
| D | 2 wt% glycine+40 mmol $l^{-1}$ TAZ + based polishing slurry |
| E | 3 wt% glycine+40 mmol $l^{-1}$ TAZ + based polishing slurry |

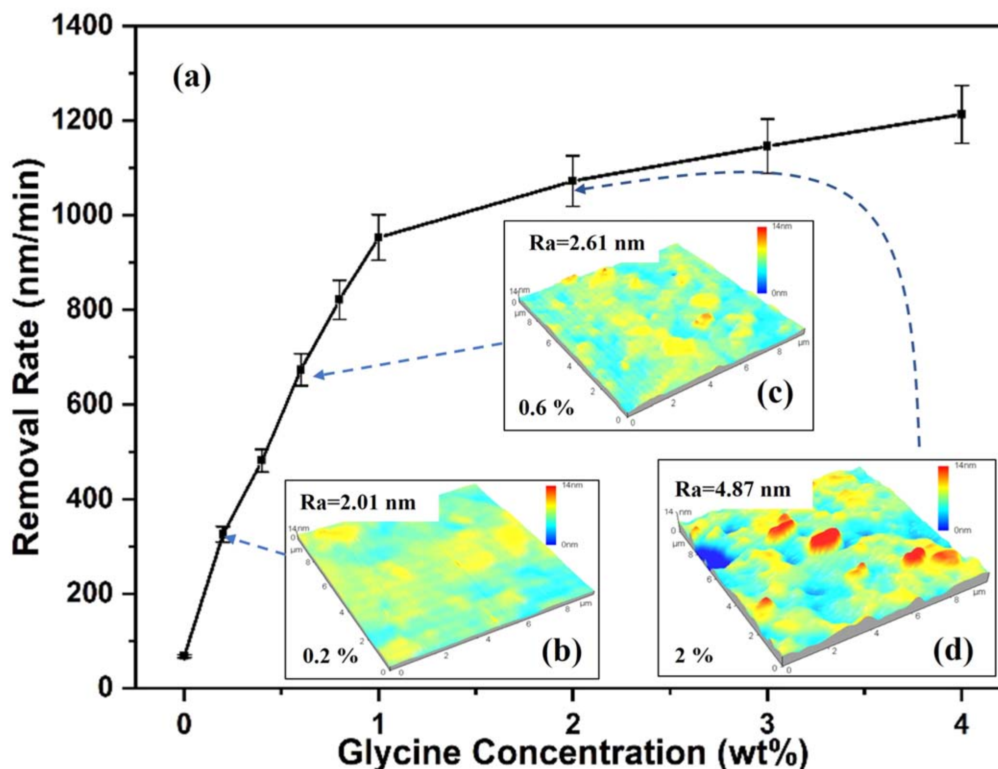


**Figure 1.** (a) Material removal rate of aluminum as a function of glycine concentration in based polishing slurry without addition of TAZ under 6.894 kPa (1 psi) of polishing pressure. (b)–(d) AFM images showing morphology of the specimen after polished with different concentrations of glycine, (b) 0.2 wt%, (c) 0.6 wt%, (d) 2 wt%.

into the basic solution (10 wt% colloidal $SiO_2$, 0.05 wt% HEC, 0.6 wt% $H_2O_2$). All the polishing slurries were adjusted by triethanolamine and HCl to pH 7.5.

Figure 2 shows the effects of these five different kinds of polishing slurry on the Al static etch rate (SER) and polishing rate. Comparing with B, C and D, E in Fig. 2, the polishing rate/SER of Al enhances with the increase in concentration of glycine. In a weak alkaline condition, the complexation reaction of glycine with Al ion can be expressed by Eqs. 2 and 3:[37]

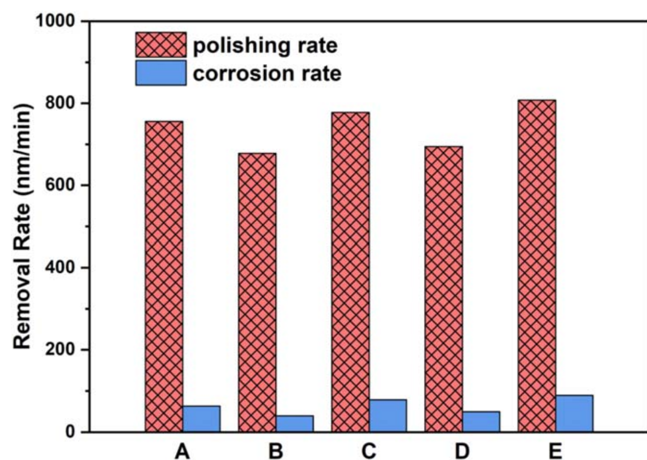


**Figure 2.** Effect of five kinds of polishing slurry containing different concentrations of glycine and TAZ on the Al SER and polishing rate, A:1 wt% glycine and 10 mmol $l^{-1}$ TAZ, B: 1 wt% glycine and 20 mmol $l^{-1}$ TAZ, C:2 wt% glycine and 20 mmol $l^{-1}$ TAZ, D:2 wt% glycine and 40 mmol $l^{-1}$ TAZ, E:3 wt% glycine and 40 mmol $l^{-1}$ TAZ.

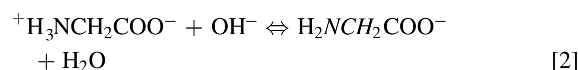

$$^{+}H_3NCH_2COO^- + OH^- \Leftrightarrow H_2NCH_2COO^- + H_2O \quad [2]$$

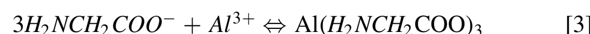

$$3H_2NCH_2COO^- + Al^{3+} \Leftrightarrow Al(H_2NCH_2COO)_3 \quad [3]$$

It is indicated that Al oxide and Al ion complex with glycine molecules, which produces glycine-Al soluble products and accelerates the rate of Al converted to Al ion during the polishing, and ultimately promotes the Al SER and polishing rate.

TAZ is a kind of low toxicity and high soluble corrosion inhibitor.[6,20] Its adsorption behaviour on the Al surface in CMP process can be explored by the isotherms, such as Frumkin, Langmuir, Freundlich and Temkin isotherms.[38] Commonly, the considerable isotherm is empirically derived on the base of fitting coverage data. The Langmuir isotherm is given by:[38]

$$c/\theta = f/K + fc \quad [4]$$

Where $c$ is the TAZ concentration (mol $l^{-1}$), $f$ is the slope and $K$ is the adsorption equilibrium constant.

The Gibbs energy of adsorption $\Delta G^0$ is written as:[26]

$$\Delta G^0 = -RT \ln \frac{1}{55.5} \ln K \quad [5]$$

Where $R$ is the gas constant as −8.314 J/(mol·K). The negative value of the Gibbs energy of adsorption indicates the spontaneity of adsorption process of TAZ on Al sheet surface. Normally, if the value of Gibbs energy is around −40 kJ $mol^{-1}$ or less, a chemisorption would happen. While those is up to −20 kJ $mol^{-1}$ suggesting a physisorption.[39] The value of Gibbs energy adsorption is calculated to be of −27.07 kJ $mol^{-1}$, which indicates mixed adsorption appears

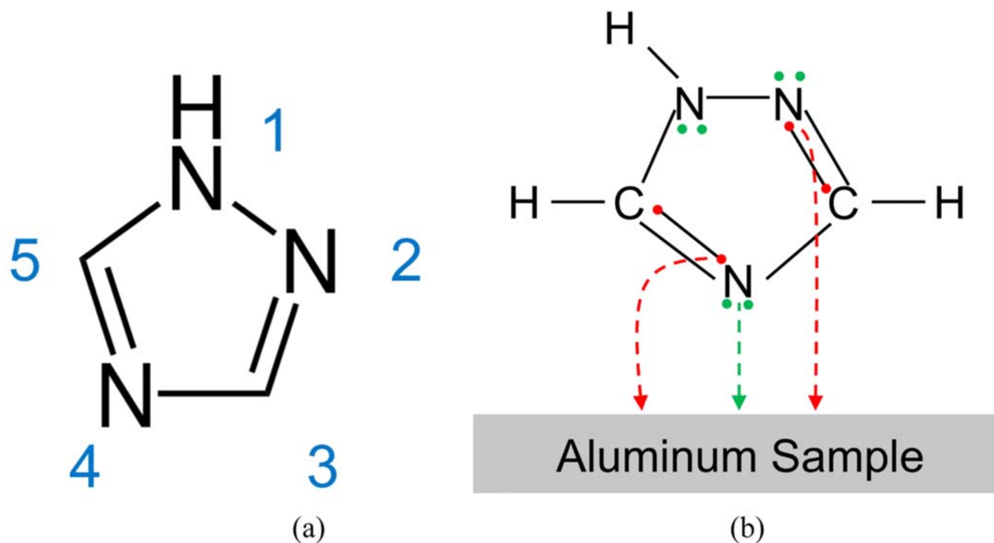


**Figure 3.** (a) Molecular structure of 1,2,4-triazole; (b) Schematic illustration of interaction between TAZ molecule and Al surface, red dots: $\pi$ electrons, green dots: lone pair electrons.

for the TAZ adsorption on Al surface. Therefore, the adsorption of TAZ on the Al surface can be considered as two steps: the first step is the physisorption process, which is possibly due to Van der Waals forces and electrostatic forces.[21] The other step chemisorption is mainly because of charge-sharing or transferring to form coordinate bonding.[40–42] And chemisorption is much stronger than physisorption, these reaction processes can be expressed as:[20,21]

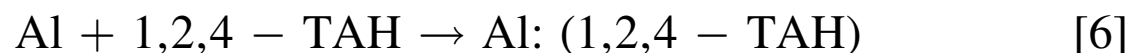

$$\text{Al} + 1,2,4 - \text{TAH} \rightarrow \text{Al: } (1,2,4 - \text{TAH}) \quad [6]$$

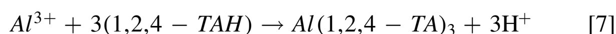

$$Al^{3+} + 3(1,2,4 - TAH) \rightarrow Al(1,2,4 - TA)_3 + 3\text{H}^+ \quad [7]$$

According to acidities of TAZ ($\text{pKa}_1 = 2.3$, $\text{pKa}_2 = 10.2$), the majority of TAZ molecules stay neutral at pH 7.5.[20] The chemisorption of TAZ molecules on Al surface may be in the following two forms: (1) via the sharing of electrons between the nitrogen and Al atom, that is, the nitrogen atom N4, which is more electronegative than other atoms in TAZ molecule, coordinates with Al atom[21,43]; (2) through $\pi$-electron interactions between the aromatic ring of TAZ and Al surface, where delocalized $\pi$ electrons of TAZ molecule rapidly enter into the empty d orbitals of Al atoms/ions, schematic illustration of the interactions between Al and TAZ is shown in Fig. 3.[22,42,44,45] When the TAZ molecules reach saturation adsorption on the Al surface, as to achieve the optimized structure, it will also carry out the rearrangement process. In this process, the strong $\pi$-$\pi$ interaction of $6\pi$ aromatic heterocycle TAZ molecules with unfilled $d\pi$ orbitals of Al atoms/ions plays a key role in the formation of a dense, orderly and stable passivation film.[22,44–47] Therefore, compared with A, B and C, D in Fig. 2, the increase in TAZ concentration leads to gradually decrease in both the SER and polishing rate. Al-TAZ film on the Al surface suppresses the corrosion of Al, weakens the chemical effect in the process of Al CMP, and eventually reduces the Al polishing rate.

The potentiodynamic polarization plots of the Al sheets in the above mentioned solutions as listed in Table I are shown in Fig. 4a. The corresponding corrosion potential ($E_{corr}$) and corrosion current ($I_{corr}$) are given in Table II. From the results, it can be seen that an increase in the TAZ and a decrease in the glycine concentration lead to the increase in $E_{corr}$, which contributes to better passivation effect.

In the Al-$H_2O_2$ system, Al sheet surface is oxidized by $H_2O_2$, forming $Al_2O_3$ and $Al(OH)_3$, which can be hydrolyzed to yield a small amount of Al ions, thereby accelerating the chemical reaction.[5,18] The relationship between the chelating agent (glycine) and corrosion inhibitor (TAZ) is competitive. On one hand, glycine would react with the Al ion/$Al_2O_3$ (Eq. 2) to form water-soluble complex, which can accelerate the dissolution of Al sheet, and thus increases the $I_{corr}$. On the other hand, TAZ can directly react with Al ion or Al atom (Eqs. 6) to form the insoluble Al-TAZ passive film, which suppresses the corrosion of Al leading to the decrease in $I_{corr}$.

As shown in Fig. 4b, three kinds of polishing slurry (A, C, E) with a similar polishing rate are selected to conduct the OCP experiments, which is applied to simulate the CMP process. The in situ OCP curves is clearly indicative of growth and removal of passivation film in the polishing process. As illustrated in Fig. 4b, with the stop of polishing, the OCP of curve A increases, suggesting the formation of passive film. It is interesting to note that a potential decrease is also observed at polishing stage, indicating the removal of passive film. However, when CMP process stops, the downtrend of OCP curves C and E strongly implies the fast Al sheet dissolution and the accumulation of dissolved Al ions in the vicinity of Al surface owing to higher amount of glycine. There is a competitive process for Al sheet film between chemical dissolution and formation. With the increase of open circuit potential, it is more difficult to remove the passivation film from the Al sheet surface. Therefore, the polishing slurry A listed in Table I shows stronger passivation effect than that of polishing slurries C and E.

**Table II. The corresponding $E_{corr}$ and $I_{corr}$ of five different kinds of polishing slurries.**

| | Slurry | | | | |
|---|---|---|---|---|---|
| | A | B | C | D | E |
| $E_{corr}$ (V) | −0.151 | −0.062 | −0.247 | −0.112 | −0.394 |
| $I_{corr}$ (A $cm^{-2}$) | $4.836 \times 10^{-7}$ | $2.268 \times 10^{-7}$ | $5.612 \times 10^{-7}$ | $2.637 \times 10^{-7}$ | $7.358 \times 10^{-7}$ |

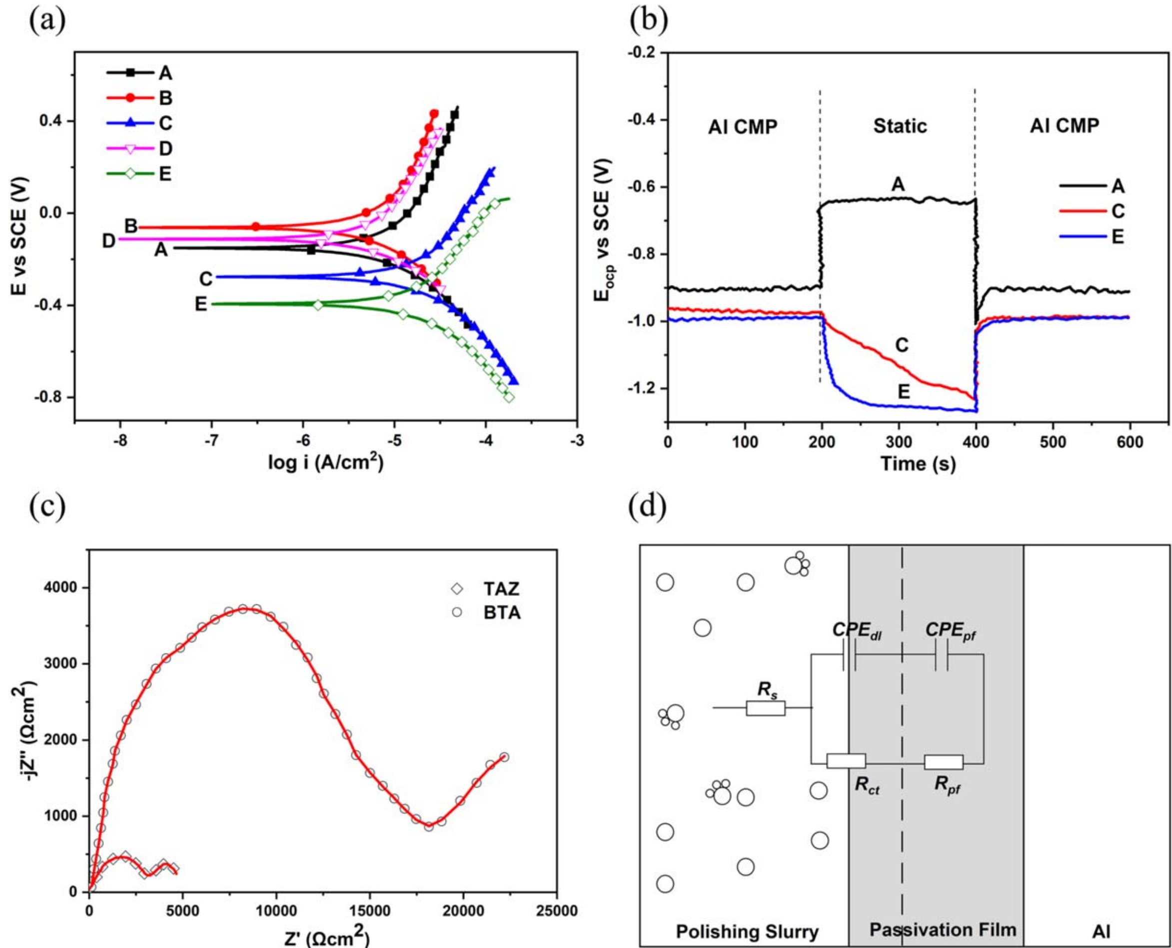


**Figure 4.** Electrochemical analysis of TAZ and glycine on Al CMP. (a) Electrochemical polarization curves of aluminum electrode measured in the five polishing slurries with a scanning rate of 5 mv $s^{-1}$ and scanning sensitivity of $10^{-6}$ A $V^{-1}$. (b) Open circuit potential curves of aluminum immersed in A, C and E polishing slurries containing different concentrations of glycine and TAZ as a function a time including CMP and static periods. (c) Nyquist impedance plots of aluminum in based polishing slurries containing 10 mmol $l^{-1}$ TAZ or BTA. (d) Electrical Equivalent circuit model used to fit the impedance data of Fig. 4c.

Electrochemical impedance spectroscopy (EIS) is an effective method to investigate the dynamics film formation of Al in CMP process.[2,10] As shown in Fig. 4c, electrochemical impedance behavior shows different trends as Al sheet immersed in slurries. The slurries are composed of 10 mmol $l^{-1}$ TAZ/BTA, 1wt% glycine and based polishing slurry (10 wt% colloidal silica, 0.05 wt% HEC, 0.6 wt% $H_2O_2$, pH = 7.5). It can be seen that BTA and TAZ could protect Al sheet from chemical dissolution. Empirically, the larger loop for BTA indicates a more passive layer relative to TAZ. However, the addition of BTA leads to the increase in frequency loop, which indicates that the passivation film formed by BTA is denser than that of TAZ. That is to say, TAZ is more feasible for the protection of Al at low polishing pressure in CMP process.

The determined equivalent electrical circuit (EEC) in Fig. 4d is applied to interpret the passivation film with the consideration of its physical structure and the best fitting results. The EEC consists of slurry resistance $R_s$ connected in series with two time constants $[(R_{ct}CPE_{dl})(R_{pf}CPE_{pf})]$.[48] Constant phase element (CPE) are employed as an non-ideal capacitance with dispersion effect to obtain more precise fitting results.[49] The impedance of CPE can be given as following equations:[10]

$$Z(CPE_{dl}) = [Y_{ct}(j\omega)^{n_1}]^{-1} \quad [8]$$

$$Z(CPE_{\mathrm{pf}}) = [Y_{\mathrm{pf}}(j\omega)^{n_2}]^{-1} \quad [9]$$

where $Y_{ct}$ and $Y_{pf}$ are frequency-independent factors; $j = (-1)^{1/2}$; $\omega$ is the angular frequency of A.C. perturbation; the value of $n_1$ represents the extent of frequency dispersion in the capacitive component of double layer charging, while $n_2$ is the measure of dispersion in the charge storage of the absorbed species. The deviation of $n_1$ and $n_2$ from 1 indicates the deviation from ideal capacitance behaviour, for $n = 1$ the CPE element reduces to an ideal capacitor, if the value is close to 0.5, it indicates that diffusion limited process are dominant.[10,50–52]

The impedance $R_s$ shows small value (only several tens of Ω), which plays no effect on the passivation system.[48] $R_{ct}$ and $CPE_{dl}$ components occurring at higher frequency represent the charge-transfer impedance and double-layer capacitance, respectively, to evaluate the delamination of the onset of corrosion at layer/substrate interface.[22,48] On the other extrem, $R_{pf}$ component appearing at lower frequency is assigned to the inhibitory layer resistance.[22,48] $CPE_{pf}$ is the inhibitory layer capacitance, which is linked with the water uptake of the coating.[48] The impedances with BAT and TAZ content are listed in Table III.

As well known, an inhibitory layer which performs well in corrosion is associated with high resistances $R_{ct}$ and $R_{pf}$, as well as lower capacitances $CPE_{dl}$ and $CPE_{pf}$.[35] The samples treated by BTA inhibitors show the highest pore resistance $R_{pf}$ and lowest capacitance $CPE_{pf}$ in Table III, which suggests that the BTA inhibitory layer improves the surface of porosity, water uptake, and interface

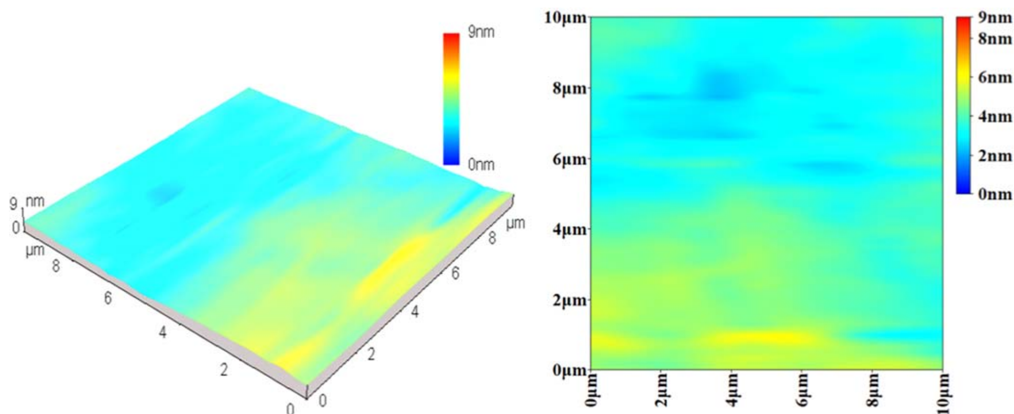


**Figure 5.** AFM image of the morphology of the specimen after polishing with slurry A showing lowest surface roughness, $R_a$ is reduced to ∼0.19 nm.

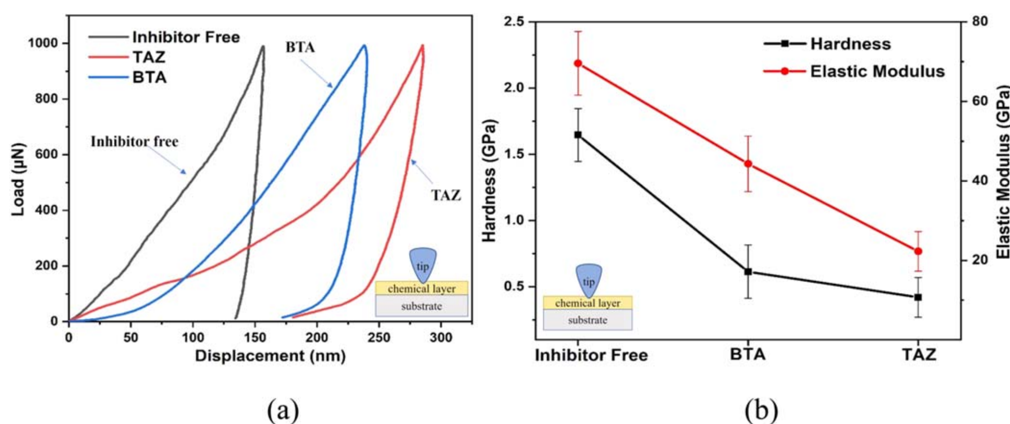


**Figure 6.** Nano-indentation of aluminum film formed in different polishing slurries. (a) Representative load-depth plots of nanoindentation on aluminum film after immersed in based polishing slurries (10 wt% colloidal silica, 0.05 wt% HEC, 0.6 wt% $H_2O_2$, pH = 7.5) adding 1 wt% glycine and different inhibitors (10 mmol $l^{-1}$ TAZ, 10 mmol $l^{-1}$ BTA or none) for 5 min (b) Hardness and elastic modulus of aluminum film obtained from data of Fig. 6a by means of the Oliver-Pharr analysis method.

delamination during corrosion process. EIS results match well with those polarization measurement data. However, as the polishing pressure is low as ∼1 psi, the BTA inhibitory layer could not be easily removed by the low mechanical force, leading to organic residual contaminants.[6,20] The surface film resistance for TAZ is an order of magnitude lower that that found for BTA. Although the TAZ inhibitory layer shows lower $R_{pf} \sim 4.568 \times 10^3\ \Omega$ compared with BTA, it still plays a well inhibitory role to protect Al surface according to the experimental data in Figs. 4a, 4c and Fig. 5, which is beneficial to enhance polishing rate because of its low mechanics properties. It is worth noting that the the capacitance $CPE_{dl}$ of TAZ film is quite large and resistances $R_{ct}$ of BTA film is quite small. It is generally considered that the capacitance $CPE_{dl}$ is related to the delamination, the phenomenon that $CPE_{dl}$ of TAZ film is quite large indicates the more serious delamination of TAZ film than BTA film.[49] As for the reason for the phenomenon that $R_{ct}$ of BTA is quite small, it's probably related to uniformity and porosity of the film, amount of water absorbed or the extent of delamination, the understanding of exact reason requires a further research.[38,52] Similar phenomenan was also reported by Stewart.[22] Finally, it should be noticed that, this equivalent circuit model only indicates a simplified manner to clarify the inhibitory layer electrochemical behavior on Al surface.

***Characteristics of TAZ film on Al surface as a week passive layer.***—Due to the synergistic effect of glycine and TAZ, polishing slurry A shows best performance in CMP process, and $R_a$ is reduced to ∼0.19 nm (Fig. 5) with the removal rate of 750 nm $min^{-1}$.

The thickness of passivation film formed by TAZ and glycine was detected by AFM before and after ultrasonically rinsed in deionized water for 10 min, as listed in Table IV. Before measuring passivation film thickness, each sample was pretreated with sandpaper (waterproof sandpaper SiC2000), ultrasonicated in ethanol for 3 min and then rinsed with deionized water, and dried in pure nitrogen. For passivation film formation, half part of the pretreated aluminium sample mounted in a holder was immersed in corresponding slurry containing 1 wt% glycine, 20 mmol $l^{-1}$ TAZ, 20 mmol $l^{-1}$ BTA, or appropriate combinations and 10 wt% $SiO_2$

**Table III. EIS Values of Al in polishing slurry A with BTA and TAZ.**

| | $R_S(\Omega)$ | $CPE_{dl}(1/\Omega)$ | $n_1$ | $R_{ct}(\Omega)$ | $CPE_{pf}(1/\Omega)$ | $n_2$ | $R_{pf}(\Omega)$ |
|---|---|---|---|---|---|---|---|
| BTA | 12.14 | 0.2285 | 0.9037 | $1.847 \times 10^{-7}$ | $8.231 \times 10^{-6}$ | 0.7946 | $2.230 \times 10^4$ |
| TAZ | 23.68 | $5.172 \times 10^5$ | 0.8724 | 35.86 | $3.174 \times 10^{-5}$ | 0.7783 | $4.658 \times 10^3$ |

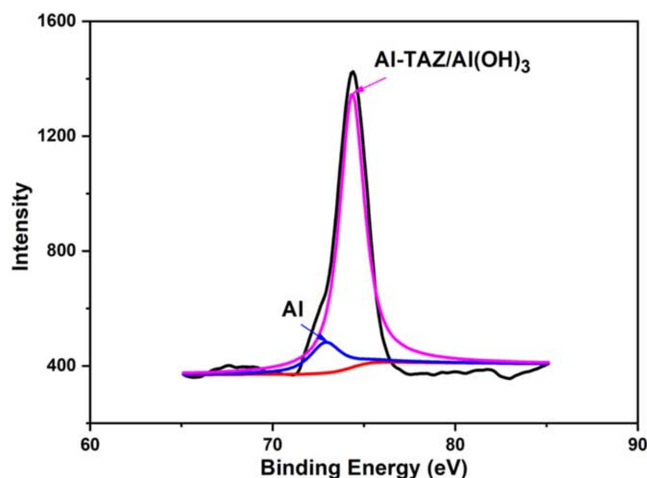


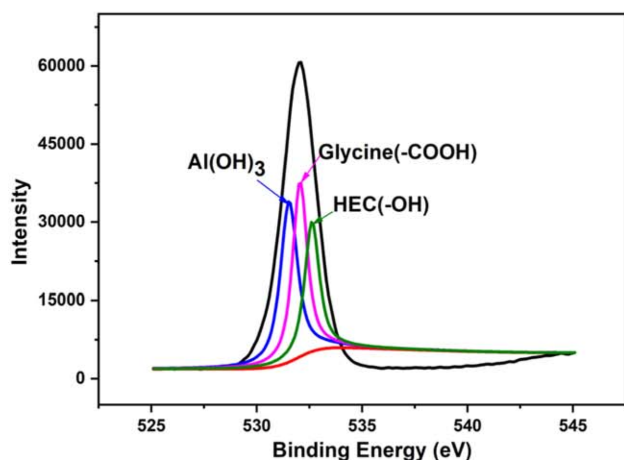


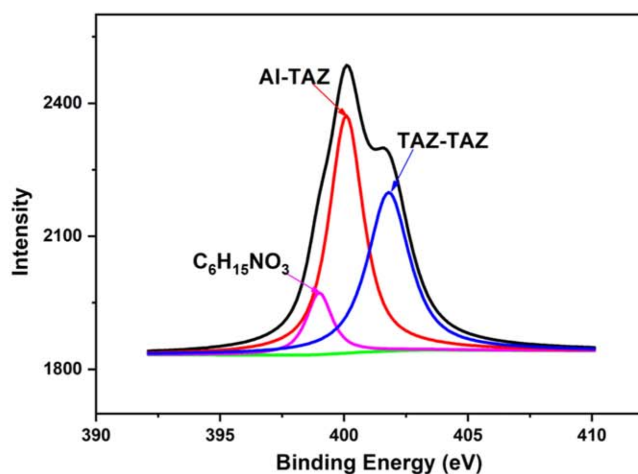


**Figure 7.** XPS spectra of Al 2p, O 1s and N 1s on aluminum surface after immersed in the polishing slurry A consisting of 10 wt% $SiO_2$, 0.05 wt% HEC, 0.06 wt% $H_2O_2$, 1wt% glycine and 10 mmol $l^{-1}$ TAZ.

for 1 h. After dried with nitrogen, the height image of the sample was taken on AFM (CSPM5000, Benyuan, China) in tapping mode, and step height $h_1$ of the film was recorded. The step height $h_1$ is the thickness of passivation film before cleaning. Likewise, after ultrasonically rinsed in deionized water for 10 min and dried, the step height $h_2$ or the thickness of passivation film after cleaning was obtained. The result of step heights are averages of 5 readings per sample and 3 samples per experimental condition. More details could be found in other literatures.[13,53]

In Table IV, after cleaning, the thickness of passivation film decreases only from 4 nm to 3 nm without BTA/TAZ addition. The thickness of passivation film can decrease from 55 nm to 26 nm with the addition of TAZ after cleaning. However, the thickness of BTA layer is only reduced from 30 nm to 28 nm, or 17 nm to 16 nm. Compared with BTA and TAZ, it is possible to estimate that TAZ forms a kind of weak passivation film on the Al sheet surface, which can be easily removed in CMP process.

Figure 6a shows the representative load-depth plots of nano-indentation on Al surface with TAZ and without TAZ. It can be seen from Fig. 6a that, the indentation of depth increases with increasing of load during indentation. By means of Oliver–Pharr method, the hardness and elastic modulus can be determined from the following equations:[54]

$$H = \frac{P_{\max}}{A} \quad [10]$$

$$E_r = \frac{\sqrt{\pi}}{2\beta}\frac{S}{\sqrt{A}} = \frac{\sqrt{\pi}}{2\beta}\frac{dP}{dh}\frac{1}{\sqrt{A}} \quad [11]$$

where $H$ is film hardness, $P_{max}$ is the maximum load (1 mN), $A$ is contact area between indenter tip and film, $E_r$ is the reduced modulus of film, $S$ is the slope of the unloading curve at the maximum indentation depth, $\beta$ is a dimensionless correction factor which is related to the shape of indenter tip ($\beta = 1.034$ is used in this paper for a triangular Berkovich punch).[54,55] Hardness and elastic modulus for various films are shown in Fig. 6b. The TAZ film shows the lowest hardness of about 0.419 Gpa and elastic modulus of about 22.284 Gpa among the test films. In addition, the film exhibits a hardness of 1.646 Gpa and elastic modulus of 65.599 without TAZ addition. It is worthy of noticing that the polishing rate is associated with the hardness and elastic modulus of the film during the polishing process. Therefore, TAZ is a promising weak corrosion inhibitor at low down pressure.

***Material removal mechanism in CMP of Al with TAZ and glycine.***—XPS was used to explore the material removal mechanism of TAZ and glycine in Al CMP. The Al sheet was immersed in polishing slurry A for 3 min. The element existence form of Al sheets was characterized by XPS to testify the chemical composition occurred in CMP process. The spectra of Al 2p, O 1 s and N 1s were analyzed. The Al 2p was shown in Fig. 7a, the peaks at the 72.85 eV and 74.2 eV correspond to Al and Al-TAZ.[56] Figure 7a represents no existence of oxidized aluminum. It is found that the addition of TAZ can inhibit the oxidation of Al. Figure 7b shows the XPS spectra of the O 1 s region. The O 1 s spectra could be fitted with three peaks respectively: one at 531.53 eV representing to $Al(OH)_3$, one at 532.05 eV corresponding to –COOH in glycine, and the peak at 532.62 eV is assigned to –OH in HEC.[57,58] As detected in Table IV, the thickness of the passivation layer is about 50 nm in addition of TAZ (20 mmol $l^{-1}$). The depth of XPS analysis is about 5 nm for metals. Thus, the TAZ film composition of specimens can be characterized by XPS. Figure 7c indicates the spectrum for N 1s. The binding energy 399.5 eV represents the existence of Al-TAZ due to the nitrogen atom on the triazole ring.[20]

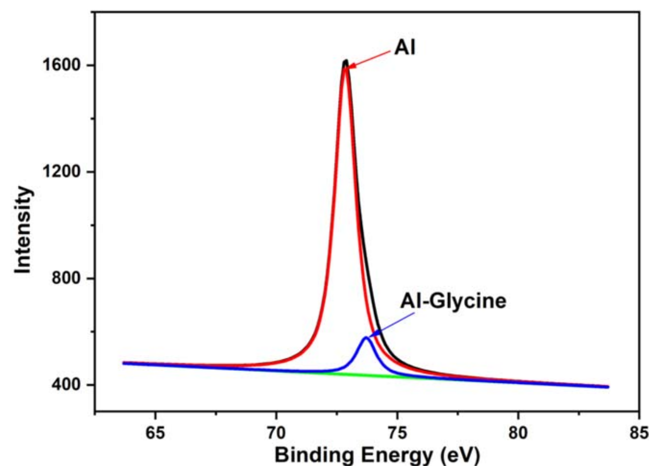


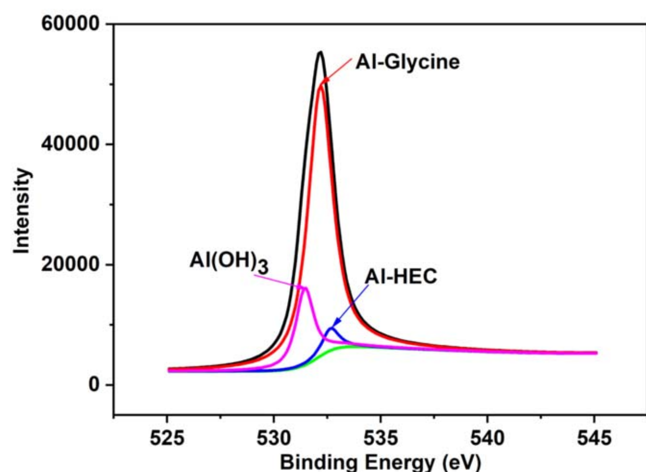


**Figure 8.** XPS spectra of Al 2p and O 1s on aluminum surface after immersed in the based slurry with 1 wt% glycine and without TAZ.

Without the addition of TAZ, the XPS Al 2p and O 1s spectra of the Al sheet surface treated with the solution (containing 10 wt% $SiO_2$, 0.05 wt% HEC, 0.06 wt% $H_2O_2$ and 1wt% glycine) are observed in Fig. 8. Al-glycine can be seen in Fig. 8 as well. Compared with Fig. 7a, it is estimated that TAZ as the corrosion inhibitor can strongly suppress the formation of Al-glycine on the Al sheet surface. With TAZ addition in the polishing slurry, the intensity of $Al(OH)_3$ increases compared with Fig. 7b.

Figure 9 presents the mechanism of planarization in Al CMP process with TAZ and glycine. In the Al-$H_2O_2$ system, the Al sheet surface will be oxidized to $Al_2O_3$/$Al(OH)_3$ firstly during the CMP process. Concurrently, TAZ will directly absorb on the Al sheet surface or to form an insoluble Al-TAZ passivation film with Al ions. Therefore, under the polishing process condition, the convex regions will endure greater friction and kinetic energy, which makes the passivation layer abraded mechanically. Moreover, glycine could be complex with Al ions to form a soluble reaction product, which can be removed away from the surface rapidly. Then a fresh surface appears and the process repeats again. However, in the concave regions, the TAZ film protects the Al sheet surface from direct dissolution. Thus, a high removal rate ratio exists between convex and concave regions in favor of achieving CMP planarization eventually.

## Conclusions

As a feasible HKMG gate material, aluminum CMP plays a significant role in the final performance of metal-oxide- semiconductor (CMOS). In this paper, the combination of TAZ and glycine are applied to compensate the low polishing pressure in CMP of Al. Synergetic effects of glycine and TAZ on material removal for CMP of Al at low down pressure was investigated in a near-netural and eco-friendly slurry by using atomic force microscope, electrochemical polarization tests, nano-indentation and X-ray photoelectron spectroscopy. It was demonstrated that, by the synergetic effect of TAZ and glycine, desirable material removal rate (750 nm $min^{-1}$) and satisfactory aluminum surface quality (0.19 nm) could be derived. The formulation of this eco-friendly slurry is 10 wt% colloidal silica, 0.05 wt% HEC, 0.6 wt% $H_2O_2$, 1 wt% glycine, 10 mmol $l^{-1}$ TAZ, the hydrochloric acid and triethanolamine (pH = 7.5).

Furthermore, the corresponding synergetic effect of TAZ and glycine on the Al CMP was investigated. And it is proposed that, the weak passive layer is physicochemical formed on surface of Al with Al-TAZ bonds, which is subsequently complexed by glycine with Al-COOH bonds. The above two synergistic parts are integrated into the material removal process during CMP of Al to compensate the decrease in removal rate resulting from the low polishing pressure. The material planarization mechanism in CMP process of Al was discussed as well. The results of this study provide a feasible

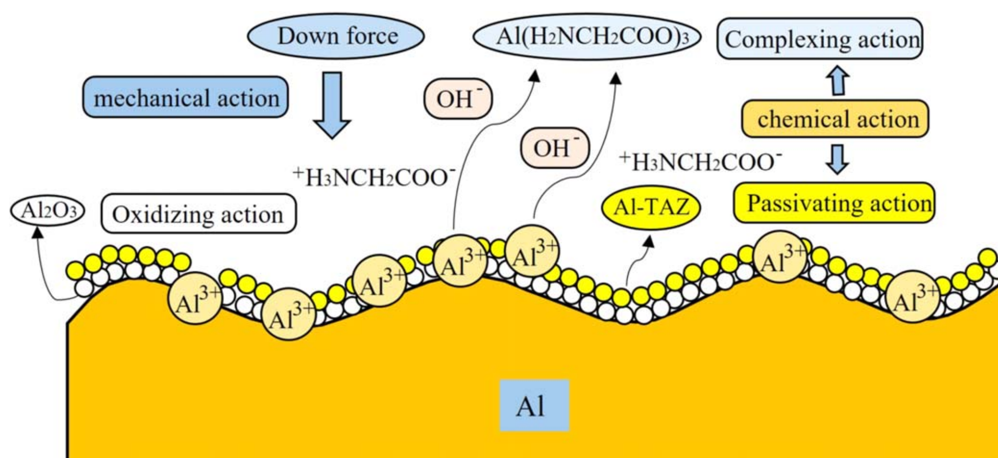


**Figure 9.** Schematic illustration of the mechanism of the planarization in aluminum CMP process with TAZ and glycine.

**Table IV. The thickness of passivation film after cleaning.**

| Slurry | Before cleaning/nm | After cleaning/nm |
|---|---|---|
| $10wt\%SiO_2 + 1wt\%glycine$ | 4 ± 2 | 3 ± 2 |
| $10wt\%SiO_2 + 20\ mmol\ l^{-1}$ TAZ | 55 ± 3 | 26 ± 2 |
| $10wt\%SiO_2 + 20\ mmol\ l^{-1}$ BTA | 30 ± 3 | 28 ± 2 |
| $10wt\%SiO_2 + 1wt\%glycine + 20\ mmol\ l^{-1}$ TAZ | 52 ± 4 | 28 ± 3 |
| $10wt\%SiO_2 + 1wt\%glycine + 20\ mmol\ l^{-1}$ BTA | 17 ± 2 | 16 ± 2 |

strategy to satisfy the low down pressure and remarkably smooth surface for Al planarization.

## Acknowledgments

This research work was financially supported by National Natural Science Foundation of China (Grant numbers: 51775360, 51501121, U1533101), China Postdoctoral Science Foundation (Grant number: 2015M571800), Jiangsu Postdoctoral Science Foundation (Grant number: 1402121C).

## ORCID

Yongguang Wang https://orcid.org/0000-0001-7686-7899

## References

1. R. Ritzenthaler et al., *IEEE Trans. Electron Devices*, **63**, 265 (2016).
2. Z. Wang, M. Sun, X. Niu, Y. Cui, J. Zhou, F. Meng, and W. Zhou, *ECS J. Solid State Sci. Technol.*, **8**, P496 (2019).
3. U. R. K. Lagudu, A. M. Chockalingam, and S. V. Babu, *ECS J. Solid State Sci. Technol.*, **2**, Q77 (2013).
4. J. M. Dysard, V. Brusic, P. Feeney, S. Grumbine, K. Moeggenborg, G. Whitener, W. J. Ward, G. Burns, and K. Choi, *ECS Trans.*, **33**, 77 (2010).
5. Y. H. Hsien, H. K. Hsu, T. C. Tsai, W. Lin, R. P. Huang, C. H. Chen, C. L. Yang, and J. Y. Wu, *Microelectron. Eng.*, **92**, 19 (2012).
6. P. Liu, Y. Wang, Y. Zhao, D. Bian, Y. Zhu, and S. Niu, *ECS J. Solid State Sci. Technol.*, **7**, P698 (2018).
7. A. Paul, K. Bello, and Deniz, U.S. Pat. 8975142B2 (2015).
8. J. Lu, T. Tsai, and S. Chang, U.S. Pat. US20190386112A1 (2019).
9. M. K. Poddar et al., *J. Mater. Sci.*, **55**, 3450 (2020).
10. Z. Wang, M. Sun, X. Niu, J. Zhou, and Y. Cui, *ECS J. Solid State Sci. Technol.*, **8**, P332 (2019).
11. J. Zhang, Y. Liu, C. Yan, and W. Zhang, *ECS J. Solid State Sci. Technol.*, **5**, P446 (2016).
12. Q. Xu and L. Chen, *ECS J. Solid State Sci. Technol.*, **4**, P101 (2015).
13. Y. Wang, Y. Zhu, D. Zhao, and D. Bian, *Appl. Surf. Sci.*, **464**, 229 (2019).
14. Y. Wang, Y. Chen, Y. Zhao, D. Zhao, Y. Zhong, F. Qi, and X. Liu, *J. Mol. Liq.*, **225**, 510 (2017).
15. C. Kallingal, D. Duquette, and S. Murarka, *J. Electrochem. Soc.*, **145**, 2074 (1998).
16. T. Zhao, H. Hu, X. Peng, C. Du, C. Guan, and J. Yong, *Appl. Opt.*, **58**, 6091 (2019).
17. N. Cha, Y. Kang, and P. J. Goo, *Korean J. Mater. Res.*, **16**, 731 (2006).
18. Y. Wang, W. Tseng, and S. Chang, *Thin Solid Films*, **474**, 36 (2005).
19. S. Lin, H. Huang, and H. Hocheng, *Thin Solid Films*, **483**, 400 (2005).
20. L. Jiang, Y. Lan, Y. He, Y. Li, Y. Li, and J. Luo, *Thin Solid Films*, **556**, 395 (2014).
21. W. Zhang, Y. Liu, C. Wang, X. Niu, J. Ji, Y. Du, and L. Han, *ECS J. Solid State Sci. Technol.*, **6**, P786 (2017).
22. K. Stewart, J. Keleher, and A. Gewirth, *J. Electrochem. Soc.*, **155**, D625 (2008).
23. Q. Xu, L. Chen, J. Fang, and F. Yang, *Microelectron. Eng.*, **131**, 58 (2015).
24. Y. Zhao and L. Chang, *Wear*, **252**, 220 (2002).
25. Y. Wang, Y. Chen, Y. Zhao, P. Min, F. Qi, X. Liu, and D. Zhao, *J. Mater. Sci., Mater. Electron.*, **28**, 3364 (2017).
26. J. Li, X. Lu, J. Ou, and J. Cheng, "Adsorption mechanism of benzotriazole on copper surface in CMP based slurries containing peroxide and glycine." *ICPT 2012—International Conference on Planarization/CMP Technology* (Grenoble, France) 297 (2012), https://ieeexplore.ieee.org/abstract/document/6353798.
27. H. Lee, D. Lee, and H. Jeong, *Int. J. Precis. Eng. Man.*, **17**, 525 (2016).
28. M. Krishnan, J. W. Nalaskowski, and L. M. Cook, *Chem. Rev.*, **110**, 178 (2010).
29. A. Shanaghi and M. Kadkhodaie, *Corros. Eng., Sci. Technol.*, **52**, 332 (2017).
30. C. Yan, Y. Liu, J. Zhang, C. Wang, W. Zhang, P. He, and G. Pan, *ECS J. Solid State Sci. Technol.*, **6**, P1 (2017).
31. T. Du, Y. Luo, and V. Desai, *Microelectron. Eng.*, **71**, 90 (2004).
32. B. Cho, S. Shima, S. Hamada, and J. Park, *Appl. Surf. Sci.*, **384**, 505 (2016).
33. D. Pillard, J. Cornell, D. Dufresne, and M. Hernandez, *Water Res.*, **35**, 557 (2001).
34. A. Katritzky, Z. Wang, M. Tsikolia, C. Hall, and M. Carman, *Tetrahedron Lett.*, **47**, 7653 (2006).
35. J. Song and W. J. V. Ooij, *J. Adhes. Sci. Technol.*, **17**, 2191 (2003).
36. Y. Wang and Y. Zhao, *Appl. Surf. Sci.*, **254**, 1517 (2007).
37. K. Ogura, K. Nakaoka, M. Nakayama, and S. Tanaka, *J. Electroanal. Chem.*, **511**, 122 (2001).
38. M. Hosseini, S. F. L. Mertens, M. Ghorbani, and M. R. Arshadi, *Mater. Chem. Phys.*, **78**, 800 (2003).
39. S. M. Milić and M. M. Antonijević, *Corros. Sci.*, **51**, 28 (2009).
40. F. Donahue and K. Nobe, *J. Electrochem. Soc.*, **112**, 886 (1965).
41. M. Zhong, S. Venkataraman, Y. Lan, Y. Li, and D. Shipp, *J. Electrochem. Soc.*, **161**, C138 (2014).
42. M. N. El-Haddad and A. S. Fouda, *J. Mol. Liq.*, **209**, 480 (2015).
43. M. Muniz-Miranda, F. Muniz-Miranda, and S. Caporali, *Beilstein J. Nanotechnol.*, **5**, 2489 (2014).
44. R. Punitha, S. D. Kirupha, S. Vivek, and L. Ravikumar, *J. Polym. Res.*, **26**, 287 (2019).
45. B. J. Vasanthi, L. Ravikumar, and A. Selvaraj, *Mater. Corros.*, **59**, 14 (2008).
46. M. Finsgar and I. Milosev, *Corros. Sci.*, **52**, 2737 (2010).
47. W. Ouellette, M. Yu, C. O'Connor, D. Hagrman, and J. Zubieta, *Angew. Chem. Int. Edit.*, **45**, 3497 (2006).
48. T. Kosec, D. Merl, and I. Milosev, *Corros. Sci.*, **50**, 1987 (2008).
49. F. Lu, B. Song, P. He, Z. Wang, and J. Wang, *RSC Adv.*, **7**, 13742 (2017).
50. R. Manivannan, B. Cho, H. Xiong, S. Ramanathan, and J. Park, *Microelectron. Eng.*, **122**, 33 (2014).
51. S. Jensen, A. Hauch, P. Hendriksen, M. Mogensen, N. Bonanos, and T. Jacobsen, *J. Electrochem. Soc.*, **154**, B1325 (2007).
52. Sudheer and M. Quraishi, *Corros. Sci.*, **70**, 161 (2013).
53. X. Wang, S. Song, L. Chen, C. M. Stafford, and J. Sun, *Acta Biomater.*, **74**, 326 (2018).
54. W. Oliver and G. Pharr, *J. Mater. Res.*, **7**, 1564 (1992).
55. Q. Kan, W. Yan, G. Kang, and Q. Sun, *J. Mech. Phys. Solids*, **61**, 2015 (2013).
56. D. Briggs and M. P. Seah, *Practical Surface Analysis* (John Wiley & Sons, New York) 2nd ed., p. 627 (1994).
57. C. Wagner, D. Passoja, H. Hillery, T. Kinisky, H. Six, W. Jansen, and J. Taylor, *J. Vac. Sci. Technol.*, **21**, 933 (1982).
58. Y. Pan, Y. Liu, X. Lu, G. Pan, and J. Luo, *J. Electrochem. Soc.*, **159**, H329 (2012).